



Measurements of B_c^+ production and mass with the $B_c^+ \rightarrow J/\psi \pi^+$ decay

The LHCb collaboration[†]

Abstract

Measurements of B_c^+ production and mass are performed with the decay mode $B_c^+ \rightarrow J/\psi \pi^+$ using 0.37 fb^{-1} of data collected in pp collisions at $\sqrt{s} = 7 \text{ TeV}$ by the LHCb experiment. The ratio of the production cross-section times branching fraction between the $B_c^+ \rightarrow J/\psi \pi^+$ and the $B^+ \rightarrow J/\psi K^+$ decays is measured to be $(0.68 \pm 0.10 \text{ (stat.)} \pm 0.03 \text{ (syst.)} \pm 0.05 \text{ (lifetime)})\%$ for B_c^+ and B^+ mesons with transverse momenta $p_T > 4 \text{ GeV}/c$ and pseudorapidities $2.5 < \eta < 4.5$. The B_c^+ mass is directly measured to be $6273.7 \pm 1.3 \text{ (stat.)} \pm 1.6 \text{ (syst.) MeV}/c^2$, and the measured mass difference with respect to the B^+ meson is $M(B_c^+) - M(B^+) = 994.6 \pm 1.3 \text{ (stat.)} \pm 0.6 \text{ (syst.) MeV}/c^2$.

Submitted to Phys. Rev. Lett.

[†]Authors are listed on the following pages.

LHCb collaboration

R. Aaij³⁸, C. Abellan Beteta^{33,n}, A. Adametz¹¹, B. Adeva³⁴, M. Adinolfi⁴³, C. Adrover⁶, A. Affolder⁴⁹, Z. Ajaltouni⁵, J. Albrecht³⁵, F. Alessio³⁵, M. Alexander⁴⁸, S. Ali³⁸, G. Alkhazov²⁷, P. Alvarez Cartelle³⁴, A.A. Alves Jr²², S. Amato², Y. Amhis³⁶, L. Anderlini^{17,f}, J. Anderson³⁷, R.B. Appleby⁵¹, O. Aquines Gutierrez¹⁰, F. Archilli^{18,35}, A. Artamonov³², M. Artuso⁵³, E. Aslanides⁶, G. Auriemma^{22,m}, S. Bachmann¹¹, J.J. Back⁴⁵, C. Baesso⁵⁴, W. Baldini¹⁶, R.J. Barlow⁵¹, C. Barschel³⁵, S. Barsuk⁷, W. Barter⁴⁴, A. Bates⁴⁸, Th. Bauer³⁸, A. Bay³⁶, J. Beddow⁴⁸, I. Bediaga¹, S. Belogurov²⁸, K. Belous³², I. Belyaev²⁸, E. Ben-Haim⁸, M. Benayoun⁸, G. Bencivenni¹⁸, S. Benson⁴⁷, J. Benton⁴³, A. Berezchnoy²⁹, R. Bernet³⁷, M.-O. Bettler⁴⁴, M. van Beuzekom³⁸, A. Bien¹¹, S. Bifani¹², T. Bird⁵¹, A. Bizzeti^{17,h}, P.M. Bjørnstad⁵¹, T. Blake³⁵, F. Blanc³⁶, C. Blanks⁵⁰, J. Blouw¹¹, S. Blusk⁵³, A. Bobrov³¹, V. Bocci²², A. Bondar³¹, N. Bondar²⁷, W. Bonivento¹⁵, S. Borghi^{48,51}, A. Borgia⁵³, T.J.V. Bowcock⁴⁹, C. Bozzi¹⁶, T. Brambach⁹, J. van den Brand³⁹, J. Bressieux³⁶, D. Brett⁵¹, M. Britsch¹⁰, T. Britton⁵³, N.H. Brook⁴³, H. Brown⁴⁹, A. Büchler-Germann³⁷, I. Burducea²⁶, A. Bursche³⁷, J. Buytaert³⁵, S. Cadeddu¹⁵, O. Callot⁷, M. Calvi^{20,j}, M. Calvo Gomez^{33,n}, A. Camboni³³, P. Campana^{18,35}, A. Carbone^{14,c}, G. Carboni^{21,k}, R. Cardinale^{19,i}, A. Cardini¹⁵, L. Carson⁵⁰, K. Carvalho Akiba², G. Casse⁴⁹, M. Cattaneo³⁵, Ch. Cauet⁹, M. Charles⁵², Ph. Charpentier³⁵, P. Chen^{3,36}, N. Chiapolini³⁷, M. Chrzaszcz²³, K. Ciba³⁵, X. Cid Vidal³⁴, G. Ciezarek⁵⁰, P.E.L. Clarke⁴⁷, M. Clemencic³⁵, H.V. Cliff⁴⁴, J. Closier³⁵, C. Coca²⁶, V. Coco³⁸, J. Cogan⁶, E. Cogneras⁵, P. Collins³⁵, A. Comerma-Montells³³, A. Contu^{52,15}, A. Cook⁴³, M. Coombes⁴³, G. Corti³⁵, B. Couturier³⁵, G.A. Cowan³⁶, D. Craik⁴⁵, S. Cunliffe⁵⁰, R. Currie⁴⁷, C. D'Ambrosio³⁵, P. David⁸, P.N.Y. David³⁸, I. De Bonis⁴, K. De Bruyn³⁸, S. De Capua^{21,k}, M. De Cian³⁷, J.M. De Miranda¹, L. De Paula², P. De Simone¹⁸, D. Decamp⁴, M. Deckenhoff⁹, H. Degaudenzi^{36,35}, L. Del Buono⁸, C. Deplano¹⁵, D. Derkach¹⁴, O. Deschamps⁵, F. Dettori³⁹, A. Di Canto¹¹, J. Dickens⁴⁴, H. Dijkstra³⁵, P. Diniz Batista¹, F. Domingo Bonal^{33,n}, S. Donleavy⁴⁹, F. Dordei¹¹, A. Dosil Suárez³⁴, D. Dossett⁴⁵, A. Dovbnya⁴⁰, F. Dupertuis³⁶, R. Dzhelyadin³², A. Dziurda²³, A. Dzyuba²⁷, S. Easo⁴⁶, U. Egede⁵⁰, V. Egorychev²⁸, S. Eidelman³¹, D. van Eijk³⁸, S. Eisenhardt⁴⁷, R. Ekelhof⁹, L. Eklund⁴⁸, I. El Rifai⁵, Ch. Elsasser³⁷, D. Elsby⁴², D. Esperante Pereira³⁴, A. Falabella^{14,e}, C. Färber¹¹, G. Fardell⁴⁷, C. Farinelli³⁸, S. Farry¹², V. Fave³⁶, V. Fernandez Albor³⁴, F. Ferreira Rodrigues¹, M. Ferro-Luzzi³⁵, S. Filippov³⁰, C. Fitzpatrick³⁵, M. Fontana¹⁰, F. Fontanelli^{19,i}, R. Forty³⁵, O. Francisco², M. Frank³⁵, C. Frei³⁵, M. Frosini^{17,f}, S. Furcas²⁰, A. Gallas Torreira³⁴, D. Galli^{14,c}, M. Gandelman², P. Gandini⁵², Y. Gao³, J-C. Garnier³⁵, J. Garofoli⁵³, P. Garosi⁵¹, J. Garra Tico⁴⁴, L. Garrido³³, C. Gaspar³⁵, R. Gauld⁵², E. Gersabeck¹¹, M. Gersabeck³⁵, T. Gershon^{45,35}, Ph. Ghez⁴, V. Gibson⁴⁴, V.V. Gligorov³⁵, C. Göbel⁵⁴, D. Golubkov²⁸, A. Golutvin^{50,28,35}, A. Gomes², H. Gordon⁵², M. Grabalosa Gándara³³, R. Graciani Diaz³³, L.A. Granado Cardoso³⁵, E. Graugés³³, G. Graziani¹⁷, A. Greco²⁶, E. Greening⁵², S. Gregson⁴⁴, O. Grünberg⁵⁵, B. Gui⁵³, E. Gushchin³⁰, Yu. Guz³², T. Gys³⁵, C. Hadjivasiliou⁵³, G. Haefeli³⁶, C. Haen³⁵, S.C. Haines⁴⁴, S. Hall⁵⁰, T. Hampson⁴³, S. Hansmann-Menzemer¹¹, N. Harnew⁵², S.T. Harnew⁴³, J. Harrison⁵¹, P.F. Harrison⁴⁵, T. Hartmann⁵⁵, J. He⁷, V. Heijne³⁸, K. Hennessy⁴⁹, P. Henrard⁵, J.A. Hernando Morata³⁴, E. van Herwijnen³⁵, E. Hicks⁴⁹, D. Hill⁵², M. Hoballah⁵, P. Hopchev⁴, W. Hulsbergen³⁸, P. Hunt⁵², T. Huse⁴⁹, N. Hussain⁵², D. Hutchcroft⁴⁹, D. Hynds⁴⁸, V. Iakovenko⁴¹, P. Ilten¹², J. Imong⁴³, R. Jacobsson³⁵, A. Jaeger¹¹, M. Jahjah Hussein⁵, E. Jans³⁸, F. Jansen³⁸, P. Jaton³⁶, B. Jean-Marie⁷, F. Jing³, M. John⁵², D. Johnson⁵², C.R. Jones⁴⁴, B. Jost³⁵, M. Kaballo⁹, S. Kandybei⁴⁰, M. Karacson³⁵,

T.M. Karbach³⁵, J. Keaveney¹², I.R. Kenyon⁴², U. Kerzel³⁵, T. Ketel³⁹, A. Keune³⁶,
 B. Khanji²⁰, Y.M. Kim⁴⁷, O. Kochebina⁷, V. Komarov^{36,29}, R.F. Koopman³⁹, P. Koppenburg³⁸,
 M. Korolev²⁹, A. Kozlinskiy³⁸, L. Kravchuk³⁰, K. Kreplin¹¹, M. Kreps⁴⁵, G. Krocker¹¹,
 P. Krokovny³¹, F. Kruse⁹, M. Kucharczyk^{20,23,j}, V. Kudryavtsev³¹, T. Kvaratskheliya^{28,35},
 V.N. La Thi³⁶, D. Lacarrere³⁵, G. Lafferty⁵¹, A. Lai¹⁵, D. Lambert⁴⁷, R.W. Lambert³⁹,
 E. Lanciotti³⁵, G. Lanfranchi^{18,35}, C. Langenbruch³⁵, T. Latham⁴⁵, C. Lazzeroni⁴², R. Le Gac⁶,
 J. van Leerdam³⁸, J.-P. Lees⁴, R. Lefèvre⁵, A. Leflat^{29,35}, J. Lefrançois⁷, O. Leroy⁶, T. Lesiak²³,
 Y. Li³, L. Li Gioi⁵, M. Liles⁴⁹, R. Lindner³⁵, C. Linn¹¹, B. Liu³, G. Liu³⁵, J. von Loeben²⁰,
 J.H. Lopes², E. Lopez Asamar³³, N. Lopez-March³⁶, H. Lu³, J. Luisier³⁶, A. Mac Raighne⁴⁸,
 F. Machefert⁷, I.V. Machikhiliyan^{4,28}, F. Maciuc²⁶, O. Maev^{27,35}, J. Magnin¹, M. Maino²⁰,
 S. Malde⁵², G. Manca^{15,d}, G. Mancinelli⁶, N. Mangiafave⁴⁴, U. Marconi¹⁴, R. Märki³⁶,
 J. Marks¹¹, G. Martellotti²², A. Martens⁸, L. Martin⁵², A. Martín Sánchez⁷, M. Martinelli³⁸,
 D. Martinez Santos³⁵, A. Massafferri¹, Z. Mathe³⁵, C. Matteuzzi²⁰, M. Matveev²⁷, E. Maurice⁶,
 A. Mazurov^{16,30,35,e}, J. McCarthy⁴², G. McGregor⁵¹, R. McNulty¹², M. Meissner¹¹, M. Merk³⁸,
 J. Merkel⁹, D.A. Milanese¹³, M.-N. Minard⁴, J. Molina Rodriguez⁵⁴, S. Monteil⁵, D. Moran⁵¹,
 P. Morawski²³, R. Mountain⁵³, I. Mous³⁸, F. Muheim⁴⁷, K. Müller³⁷, R. Muresan²⁶, B. Muryn²⁴,
 B. Muster³⁶, J. Mylroie-Smith⁴⁹, P. Naik⁴³, T. Nakada³⁶, R. Nandakumar⁴⁶, I. Nasteva¹,
 M. Needham⁴⁷, N. Neufeld³⁵, A.D. Nguyen³⁶, C. Nguyen-Mau^{36,o}, M. Nicol⁷, V. Niess⁵,
 N. Nikitin²⁹, T. Nikodem¹¹, A. Nomerotski^{52,35}, A. Novoselov³², A. Oblakowska-Mucha²⁴,
 V. Obraztsov³², S. Oggero³⁸, S. Ogilvy⁴⁸, O. Okhrimenko⁴¹, R. Oldeman^{15,d,35}, M. Orlandea²⁶,
 J.M. Otalora Goicochea², P. Owen⁵⁰, B.K. Pal⁵³, A. Palano^{13,b}, M. Palutan¹⁸, J. Panman³⁵,
 A. Papanestis⁴⁶, M. Pappagallo⁴⁸, C. Parkes⁵¹, C.J. Parkinson⁵⁰, G. Passaleva¹⁷, G.D. Patel⁴⁹,
 M. Patel⁵⁰, G.N. Patrick⁴⁶, C. Patrignani^{19,i}, C. Pavel-Nicorescu²⁶, A. Pazos Alvarez³⁴,
 A. Pellegrino³⁸, G. Penso^{22,l}, M. Pepe Altarelli³⁵, S. Perazzini^{14,c}, D.L. Perego^{20,j},
 E. Perez Trigo³⁴, A. Pérez-Calero Yzquierdo³³, P. Perret⁵, M. Perrin-Terrin⁶, G. Pessina²⁰,
 K. Petridis⁵⁰, A. Petrolini^{19,i}, A. Phan⁵³, E. Picatoste Olloqui³³, B. Pie Valls³³, B. Pietrzyk⁴,
 T. Pilar⁴⁵, D. Pinci²², S. Playfer⁴⁷, M. Plo Casasus³⁴, F. Polci⁸, G. Polok²³, A. Poluektov^{45,31},
 E. Polcarpo², D. Popov¹⁰, B. Popovici²⁶, C. Potterat³³, A. Powell⁵², J. Prisciandaro³⁶,
 V. Pugatch⁴¹, A. Puig Navarro³⁶, W. Qian³, J.H. Rademacker⁴³, B. Rakotomiaramananana³⁶,
 M.S. Rangel², I. Raniuk⁴⁰, N. Rauschmayr³⁵, G. Raven³⁹, S. Redford⁵², M.M. Reid⁴⁵,
 A.C. dos Reis¹, S. Ricciardi⁴⁶, A. Richards⁵⁰, K. Rinnert⁴⁹, V. Rives Molina³³,
 D.A. Roa Romero⁵, P. Robbe⁷, E. Rodrigues^{48,51}, P. Rodriguez Perez³⁴, G.J. Rogers⁴⁴,
 S. Roiser³⁵, V. Romanovsky³², A. Romero Vidal³⁴, J. Rouvinet³⁶, T. Ruf³⁵, H. Ruiz³³,
 G. Sabatino^{21,k}, J.J. Saborido Silva³⁴, N. Sagidova²⁷, P. Sail⁴⁸, B. Saitta^{15,d}, C. Salzmann³⁷,
 B. Sanmartin Sedes³⁴, M. Sannino^{19,i}, R. Santacesaria²², C. Santamarina Rios³⁴, R. Santinelli³⁵,
 E. Santovetti^{21,k}, M. Sapunov⁶, A. Sarti^{18,l}, C. Satriano^{22,m}, A. Satta²¹, M. Savrie^{16,e},
 P. Schaack⁵⁰, M. Schiller³⁹, H. Schindler³⁵, S. Schleich⁹, M. Schlupp⁹, M. Schmelling¹⁰,
 B. Schmidt³⁵, O. Schneider³⁶, A. Schopper³⁵, M.-H. Schune⁷, R. Schwemmer³⁵, B. Sciascia¹⁸,
 A. Sciubba^{18,l}, M. Seco³⁴, A. Semennikov²⁸, K. Senderowska²⁴, I. Sepp⁵⁰, N. Serra³⁷,
 J. Serrano⁶, P. Seyfert¹¹, M. Shapkin³², I. Shapoval^{40,35}, P. Shatalov²⁸, Y. Shcheglov²⁷,
 T. Shears^{49,35}, L. Shekhtman³¹, O. Shevchenko⁴⁰, V. Shevchenko²⁸, A. Shires⁵⁰,
 R. Silva Coutinho⁴⁵, T. Skwarnicki⁵³, N.A. Smith⁴⁹, E. Smith^{52,46}, M. Smith⁵¹, K. Sobczak⁵,
 F.J.P. Soler⁴⁸, F. Soomro^{18,35}, D. Souza⁴³, B. Souza De Paula², B. Spaan⁹, A. Sparkes⁴⁷,
 P. Spradlin⁴⁸, F. Stagni³⁵, S. Stahl¹¹, O. Steinkamp³⁷, S. Stoica²⁶, S. Stone⁵³, B. Storaci³⁸,
 M. Straticiu²⁶, U. Straumann³⁷, V.K. Subbiah³⁵, S. Swientek⁹, M. Szczekowski²⁵,
 P. Szczypka^{36,35}, T. Szumlak²⁴, S. T'Jampens⁴, M. Teklishyn⁷, E. Teodorescu²⁶, F. Teubert³⁵,

C. Thomas⁵², E. Thomas³⁵, J. van Tilburg¹¹, V. Tisserand⁴, M. Tobin³⁷, S. Tol³⁹, D. Tonelli³⁵, S. Topp-Joergensen⁵², N. Torr⁵², E. Tournefier^{4,50}, S. Tourneur³⁶, M.T. Tran³⁶, A. Tsaregorodtsev⁶, P. Tsopelas³⁸, N. Tuning³⁸, M. Ubada Garcia³⁵, A. Ukleja²⁵, D. Urner⁵¹, U. Uwer¹¹, V. Vagnoni¹⁴, G. Valenti¹⁴, R. Vazquez Gomez³³, P. Vazquez Regueiro³⁴, S. Vecchi¹⁶, J.J. Velthuis⁴³, M. Veltri^{17,g}, G. Veneziano³⁶, M. Vesterinen³⁵, B. Viaud⁷, I. Videau⁷, D. Vieira², X. Vilasis-Cardona^{33,n}, J. Visniakov³⁴, A. Vollhardt³⁷, D. Volyansky¹⁰, D. Voong⁴³, A. Vorobyev²⁷, V. Vorobyev³¹, H. Voss¹⁰, C. Voß⁵⁵, R. Waldi⁵⁵, R. Wallace¹², S. Wandernoth¹¹, J. Wang⁵³, D.R. Ward⁴⁴, N.K. Watson⁴², A.D. Webber⁵¹, D. Websdale⁵⁰, M. Whitehead⁴⁵, J. Wicht³⁵, D. Wiedner¹¹, L. Wiggers³⁸, G. Wilkinson⁵², M.P. Williams^{45,46}, M. Williams^{50,p}, F.F. Wilson⁴⁶, J. Wishahi⁹, M. Witek^{23,35}, W. Witzeling³⁵, S.A. Wotton⁴⁴, S. Wright⁴⁴, S. Wu³, K. Wyllie³⁵, Y. Xie⁴⁷, F. Xing⁵², Z. Xing⁵³, Z. Yang³, R. Young⁴⁷, X. Yuan³, O. Yushchenko³², M. Zangoli¹⁴, M. Zavertyaev^{10,a}, F. Zhang³, L. Zhang⁵³, W.C. Zhang¹², Y. Zhang³, A. Zhelezov¹¹, L. Zhong³, A. Zvyagin³⁵.

¹ *Centro Brasileiro de Pesquisas Físicas (CBPF), Rio de Janeiro, Brazil*

² *Universidade Federal do Rio de Janeiro (UFRJ), Rio de Janeiro, Brazil*

³ *Center for High Energy Physics, Tsinghua University, Beijing, China*

⁴ *LAPP, Université de Savoie, CNRS/IN2P3, Annecy-Le-Vieux, France*

⁵ *Clermont Université, Université Blaise Pascal, CNRS/IN2P3, LPC, Clermont-Ferrand, France*

⁶ *CPPM, Aix-Marseille Université, CNRS/IN2P3, Marseille, France*

⁷ *LAL, Université Paris-Sud, CNRS/IN2P3, Orsay, France*

⁸ *LPNHE, Université Pierre et Marie Curie, Université Paris Diderot, CNRS/IN2P3, Paris, France*

⁹ *Fakultät Physik, Technische Universität Dortmund, Dortmund, Germany*

¹⁰ *Max-Planck-Institut für Kernphysik (MPIK), Heidelberg, Germany*

¹¹ *Physikalisches Institut, Ruprecht-Karls-Universität Heidelberg, Heidelberg, Germany*

¹² *School of Physics, University College Dublin, Dublin, Ireland*

¹³ *Sezione INFN di Bari, Bari, Italy*

¹⁴ *Sezione INFN di Bologna, Bologna, Italy*

¹⁵ *Sezione INFN di Cagliari, Cagliari, Italy*

¹⁶ *Sezione INFN di Ferrara, Ferrara, Italy*

¹⁷ *Sezione INFN di Firenze, Firenze, Italy*

¹⁸ *Laboratori Nazionali dell'INFN di Frascati, Frascati, Italy*

¹⁹ *Sezione INFN di Genova, Genova, Italy*

²⁰ *Sezione INFN di Milano Bicocca, Milano, Italy*

²¹ *Sezione INFN di Roma Tor Vergata, Roma, Italy*

²² *Sezione INFN di Roma La Sapienza, Roma, Italy*

²³ *Henryk Niewodniczanski Institute of Nuclear Physics Polish Academy of Sciences, Kraków, Poland*

²⁴ *AGH University of Science and Technology, Kraków, Poland*

²⁵ *National Center for Nuclear Research (NCBJ), Warsaw, Poland*

²⁶ *Horia Hulubei National Institute of Physics and Nuclear Engineering, Bucharest-Magurele, Romania*

²⁷ *Petersburg Nuclear Physics Institute (PNPI), Gatchina, Russia*

²⁸ *Institute of Theoretical and Experimental Physics (ITEP), Moscow, Russia*

²⁹ *Institute of Nuclear Physics, Moscow State University (SINP MSU), Moscow, Russia*

³⁰ *Institute for Nuclear Research of the Russian Academy of Sciences (INR RAN), Moscow, Russia*

³¹ *Budker Institute of Nuclear Physics (SB RAS) and Novosibirsk State University, Novosibirsk, Russia*

³² *Institute for High Energy Physics (IHEP), Protvino, Russia*

³³ *Universitat de Barcelona, Barcelona, Spain*

³⁴ *Universidad de Santiago de Compostela, Santiago de Compostela, Spain*

³⁵ *European Organization for Nuclear Research (CERN), Geneva, Switzerland*

³⁶ *Ecole Polytechnique Fédérale de Lausanne (EPFL), Lausanne, Switzerland*

- ³⁷ *Physik-Institut, Universität Zürich, Zürich, Switzerland*
- ³⁸ *Nikhef National Institute for Subatomic Physics, Amsterdam, The Netherlands*
- ³⁹ *Nikhef National Institute for Subatomic Physics and VU University Amsterdam, Amsterdam, The Netherlands*
- ⁴⁰ *NSC Kharkiv Institute of Physics and Technology (NSC KIPT), Kharkiv, Ukraine*
- ⁴¹ *Institute for Nuclear Research of the National Academy of Sciences (KINR), Kyiv, Ukraine*
- ⁴² *University of Birmingham, Birmingham, United Kingdom*
- ⁴³ *H.H. Wills Physics Laboratory, University of Bristol, Bristol, United Kingdom*
- ⁴⁴ *Cavendish Laboratory, University of Cambridge, Cambridge, United Kingdom*
- ⁴⁵ *Department of Physics, University of Warwick, Coventry, United Kingdom*
- ⁴⁶ *STFC Rutherford Appleton Laboratory, Didcot, United Kingdom*
- ⁴⁷ *School of Physics and Astronomy, University of Edinburgh, Edinburgh, United Kingdom*
- ⁴⁸ *School of Physics and Astronomy, University of Glasgow, Glasgow, United Kingdom*
- ⁴⁹ *Oliver Lodge Laboratory, University of Liverpool, Liverpool, United Kingdom*
- ⁵⁰ *Imperial College London, London, United Kingdom*
- ⁵¹ *School of Physics and Astronomy, University of Manchester, Manchester, United Kingdom*
- ⁵² *Department of Physics, University of Oxford, Oxford, United Kingdom*
- ⁵³ *Syracuse University, Syracuse, NY, United States*
- ⁵⁴ *Pontificia Universidade Católica do Rio de Janeiro (PUC-Rio), Rio de Janeiro, Brazil, associated to ²*
- ⁵⁵ *Institut für Physik, Universität Rostock, Rostock, Germany, associated to ¹¹*
- ^a *P.N. Lebedev Physical Institute, Russian Academy of Science (LPI RAS), Moscow, Russia*
- ^b *Università di Bari, Bari, Italy*
- ^c *Università di Bologna, Bologna, Italy*
- ^d *Università di Cagliari, Cagliari, Italy*
- ^e *Università di Ferrara, Ferrara, Italy*
- ^f *Università di Firenze, Firenze, Italy*
- ^g *Università di Urbino, Urbino, Italy*
- ^h *Università di Modena e Reggio Emilia, Modena, Italy*
- ⁱ *Università di Genova, Genova, Italy*
- ^j *Università di Milano Bicocca, Milano, Italy*
- ^k *Università di Roma Tor Vergata, Roma, Italy*
- ^l *Università di Roma La Sapienza, Roma, Italy*
- ^m *Università della Basilicata, Potenza, Italy*
- ⁿ *LIFAEELS, La Salle, Universitat Ramon Llull, Barcelona, Spain*
- ^o *Hanoi University of Science, Hanoi, Viet Nam*
- ^p *Massachusetts Institute of Technology, Cambridge, MA, United States*

The B_c^+ meson is unique in the Standard Model as it is the ground state of a family of mesons containing two different heavy flavour quarks. At the 7 TeV LHC centre-of-mass energy, the most probable way to produce $B_c^{(*)+}$ mesons is through the gg -fusion process, $gg \rightarrow B_c^{(*)+} + b + \bar{c}$ [1]. The production cross-section of the B_c^+ meson has been calculated by a complete order- α_s^4 approach and using the fragmentation approach [1]. It is predicted to be about $0.4 \mu\text{b}$ [2, 3] at $\sqrt{s} = 7$ TeV including contributions from excited states. This is one order of magnitude higher than that predicted at the Tevatron energy $\sqrt{s} = 1.96$ TeV. However, the theoretical predictions suffer from large uncertainties, and an accurate measurement of the B_c^+ production cross-section is needed to guide experimental studies at the LHC. As is the case for heavy quarkonia, the mass of the B_c^+ meson can be calculated by means of potential models and lattice QCD, and early predictions lay in the range from $6.2 - 6.4 \text{ GeV}/c^2$ [1]. The inclusion of charge conjugate modes is implied throughout this Letter.

The B_c^+ meson was first observed in the semileptonic decay mode $B_c^+ \rightarrow J/\psi(\mu^+\mu^-)\ell^+X$ ($\ell = e, \mu$) by CDF [4]. The production cross-section times branching fraction for this decay relative to that for $B^+ \rightarrow J/\psi K^+$ was measured to be $0.132_{-0.037}^{+0.041}(\text{stat.}) \pm 0.031(\text{syst.})_{-0.020}^{+0.032}(\text{lifetime})$ for B_c^+ and B^+ mesons with transverse momenta $p_T > 6 \text{ GeV}/c$ and rapidities $|y| < 1$. Measurements of the B_c^+ mass by CDF [5] and D0 [6] using the fully reconstructed decay $B_c^+ \rightarrow J/\psi(\mu^+\mu^-)\pi^+$ gave $M(B_c^+) = 6275.6 \pm 2.9(\text{stat.}) \pm 2.5(\text{syst.}) \text{ MeV}/c^2$ and $M(B_c^+) = 6300 \pm 14(\text{stat.}) \pm 5(\text{syst.}) \text{ MeV}/c^2$, respectively. A more precise measurement of the B_c^+ mass would allow for more stringent tests of predictions from potential models and lattice QCD calculations.

In this Letter, we present a measurement of the ratio of the production cross-section times branching fraction of $B_c^+ \rightarrow J/\psi \pi^+$ relative to that for $B^+ \rightarrow J/\psi K^+$ for B_c^+ and B^+ mesons with transverse momenta $p_T > 4 \text{ GeV}/c$ and pseudorapidities $2.5 < \eta < 4.5$, and a measurement of the B_c^+ mass. These measurements are performed using 0.37 fb^{-1} of data collected in pp collisions at $\sqrt{s} = 7$ TeV by the LHCb experiment. The LHCb detector [7] is a single-arm forward spectrometer covering the pseudorapidity range $2 < \eta < 5$, designed for the study of particles containing b or c quarks. The detector includes a high precision tracking system consisting of a silicon-strip vertex detector surrounding the pp interaction region, a large-area silicon-strip detector located upstream of a dipole magnet with a bending power of about 4 Tm , and three stations of silicon-strip detectors and straw drift-tubes placed downstream. The combined tracking system has a momentum resolution $\Delta p/p$ that varies from 0.4% at $5 \text{ GeV}/c$ to 0.6% at $100 \text{ GeV}/c$, and an impact parameter (IP) resolution of $20 \mu\text{m}$ for tracks with high transverse momentum. Charged hadrons are identified using two ring-imaging Cherenkov detectors. Photon, electron and hadron candidates are identified by a calorimeter system consisting of scintillating-pad and pre-shower detectors, an electromagnetic calorimeter and a hadronic calorimeter. Muons are identified by a muon system composed of alternating layers of iron and multiwire proportional chambers. The muon identification efficiency is about 97% , with a misidentification probability $\epsilon(\pi \rightarrow \mu) \sim 3\%$.

The $B_c^+ \rightarrow J/\psi \pi^+$ and $B^+ \rightarrow J/\psi K^+$ decay modes are topologically identical and are selected with requirements as similar as possible to each other. Events are selected by a

trigger system consisting of a hardware stage, based on information from the calorimeter and muon systems, followed by a software stage which applies a full event reconstruction. At the hardware trigger stage, events are selected by requiring a single muon candidate or a pair of muon candidates with high transverse momenta. At the software trigger stage [8, 9], events are selected by requiring a pair of muon candidates with invariant mass within $120 \text{ MeV}/c^2$ of the J/ψ mass [10], or a two- or three-track secondary vertex with a large track p_T sum, a significant displacement from the primary interaction, and at least one track identified as a muon.

At the offline selection stage, J/ψ candidates are formed from pairs of oppositely charged tracks with transverse momenta $p_T > 0.9 \text{ GeV}/c$ and identified as muons. The two muons are required to originate from a common vertex. Candidates with a dimuon invariant mass between $3.04 \text{ GeV}/c^2$ and $3.14 \text{ GeV}/c^2$ are combined with charged hadrons with $p_T > 1.5 \text{ GeV}/c$ to form the B_c^+ and B^+ meson candidates. The J/ψ mass window is about seven times larger than the mass resolution. No particle identification is used in the selection of the hadrons. To improve the B_c^+ and B^+ mass resolutions, the mass of the $\mu^+\mu^-$ pair is constrained to the J/ψ mass [10]. The b -hadron candidates are required to have $p_T > 4 \text{ GeV}/c$, decay time $t > 0.25 \text{ ps}$ and pseudorapidity in the range $2.5 < \eta < 4.5$. The fiducial region is chosen to be well inside the detector acceptance to have a reasonably flat efficiency over the phase space. To further suppress background to the B_c^+ decay, the IP χ^2 values of the J/ψ and π^+ candidates with respect to any primary vertex (PV) in the event are required to be larger than 4 and 25, respectively. The IP χ^2 is defined as the difference between the χ^2 of the PV reconstructed with and without the considered particle. The IP χ^2 of the B_c^+ candidates with respect to at least one PV in the event is required to be less than 25. After all selection requirements are applied, no event has more than one candidate for the $B_c^+ \rightarrow J/\psi \pi^+$ decay, and less than 1% of the events have more than one candidate for the $B^+ \rightarrow J/\psi K^+$ decay. Such multiple candidates are retained and treated the same as other candidates; the associated systematic uncertainty is negligible.

The ratio of the production cross-section times branching fraction measured in this analysis is

$$\begin{aligned}
 R_{c/u} &= \frac{\sigma(B_c^+) \mathcal{B}(B_c^+ \rightarrow J/\psi \pi^+)}{\sigma(B^+) \mathcal{B}(B^+ \rightarrow J/\psi K^+)} \\
 &= \frac{N(B_c^+ \rightarrow J/\psi \pi^+)}{\epsilon_{\text{tot}}^c} \frac{\epsilon_{\text{tot}}^u}{N(B^+ \rightarrow J/\psi K^+)},
 \end{aligned} \tag{1}$$

where $\sigma(B_c^+)$ and $\sigma(B^+)$ are the inclusive production cross-sections of the B_c^+ and B^+ mesons in pp collisions at $\sqrt{s} = 7 \text{ TeV}$, $\mathcal{B}(B_c^+ \rightarrow J/\psi \pi^+)$ and $\mathcal{B}(B^+ \rightarrow J/\psi K^+)$ are the branching fractions of the reconstructed decay chains, $N(B_c^+ \rightarrow J/\psi \pi^+)$ and $N(B^+ \rightarrow J/\psi K^+)$ are the yields of the $B_c^+ \rightarrow J/\psi \pi^+$ and $B^+ \rightarrow J/\psi K^+$ signal decays, and ϵ_{tot}^c , ϵ_{tot}^u are the total efficiencies, including geometrical acceptance, reconstruction, selection and trigger effects.

The signal event yields are obtained from extended unbinned maximum likelihood fits to the invariant mass distributions of the reconstructed B_c^+ and B^+ candidates in the interval

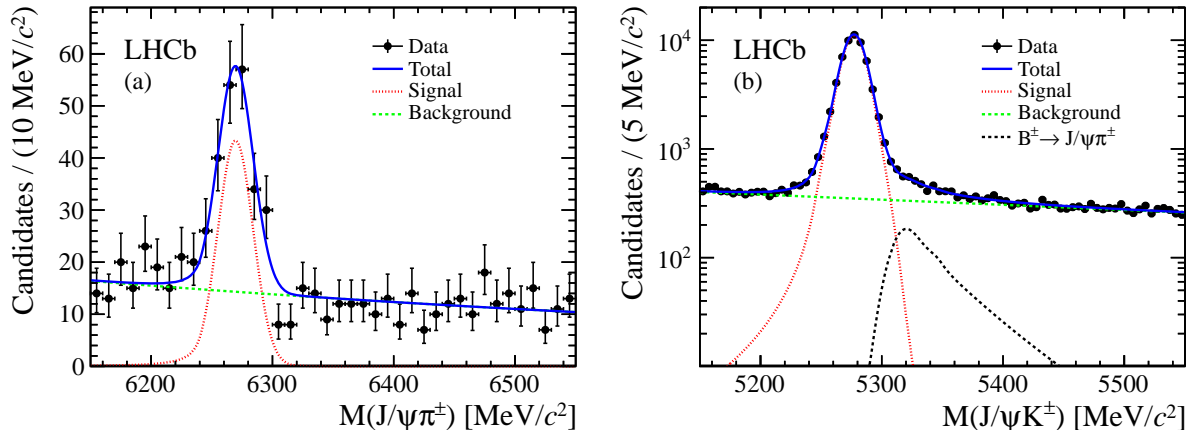


Figure 1: Invariant mass distributions of selected (a) $B_c^+ \rightarrow J/\psi \pi^+$ candidates and (b) $B^+ \rightarrow J/\psi K^+$ candidates, used in the production measurement. The fits to the data are superimposed.

$6.15 < M(J/\psi \pi^+) < 6.55 \text{ GeV}/c^2$ for B_c^+ candidates and $5.15 < M(J/\psi K^+) < 5.55 \text{ GeV}/c^2$ for B^+ candidates. The $B_c^+ \rightarrow J/\psi \pi^+$ signal mass shape is described by a double-sided Crystal Ball function [11]. The power law behaviour toward low mass is due primarily to final state radiation (FSR) from the bachelor hadron, whereas the high mass tail is mainly due to FSR from the muons in combination with the J/ψ mass constraint. The $B^+ \rightarrow J/\psi K^+$ signal mass shape is described by the sum of two double-sided Crystal Ball functions that share the same mean but have different resolutions. From simulated decays, it is found that the tail parameters of the double-sided Crystal Ball function depend mildly on the mass resolution. This functional dependence is determined from simulation and included in the mass fit. The combinatorial background is described by an exponential function. Background to $B^+ \rightarrow J/\psi K^+$ from the Cabibbo-suppressed decay $B^+ \rightarrow J/\psi \pi^+$ is included to improve the fit quality. The distribution is determined from the simulated events. The ratio of the number of $B^+ \rightarrow J/\psi \pi^+$ decays to that of the signal is fixed to $\mathcal{B}(B^+ \rightarrow J/\psi \pi^+)/\mathcal{B}(B^+ \rightarrow J/\psi K^+) = 3.83\%$ [12]. The Cabibbo-suppressed decay $B_c^+ \rightarrow J/\psi K^+$ is neglected as a source of background to the $B_c^+ \rightarrow J/\psi \pi^+$ decay. The invariant mass distributions of the selected $B_c^+ \rightarrow J/\psi \pi^+$ and $B^+ \rightarrow J/\psi K^+$ candidates and the fits to the data are shown in Fig. 1. The numbers of signal events are 162 ± 18 for $B_c^+ \rightarrow J/\psi \pi^+$ and $56\,243 \pm 256$ for $B^+ \rightarrow J/\psi K^+$, as obtained from the fits. The goodness of fits is checked with a χ^2 test, which returns a probability of 97% for $B_c^+ \rightarrow J/\psi \pi^+$ and 87% for $B^+ \rightarrow J/\psi K^+$.

The efficiencies, including geometrical acceptance, reconstruction, selection and trigger effects are determined using simulated signal events. The production of the B^+ meson is simulated using PYTHIA 6.4 [13] with the configuration described in Ref. [14]. A dedicated generator BCVEGPy [15] is used to simulate the B_c^+ meson production. Decays of B_c^+ , B^+ and J/ψ mesons are described by EVTGEN [16] in which final state radiation is generated using PHOTOS [17]. The decay products are traced through the detector by the GEANT4 package [18] as described in Ref. [19]. As the efficiencies depend on p_T and

η , the efficiencies from the simulation are binned in these variables to avoid a bias. The signal yield in each bin is obtained from data by subtracting the background contribution using the *sPlot* technique [20], where the signal and background mass shapes are assumed to be uncorrelated with p_T and η . The efficiency-corrected numbers of $B_c^+ \rightarrow J/\psi \pi^+$ and $B^+ \rightarrow J/\psi K^+$ signal decays are 2470 ± 350 and $364\,188 \pm 2270$, respectively, corresponding to a ratio of $R_{c/u} = (0.68 \pm 0.10)\%$, where the uncertainties are statistical only.

The systematic uncertainties related to the determination of the signal yields and efficiencies are described in the following. Concerning the former, studies of simulated events show that effects due to the fit model on the measured ratio $R_{c/u}$ can be as much as 1%, which is taken as systematic uncertainty. The uncertainties from the contamination due to the Cabibbo-suppressed decays are found to be negligible.

The uncertainties on the determination of the efficiencies are dominated by the knowledge of the B_c^+ lifetime, which has been measured by CDF [21] and D0 [22] to give $\tau(B_c^+) = 0.453 \pm 0.041$ ps [10]. The distributions of the $B_c^+ \rightarrow J/\psi \pi^+$ simulated events have been reweighted after changing the B_c^+ lifetime by one standard deviation around its mean value and the efficiencies are recomputed. The relative difference of 7.3% between the recomputed efficiencies and the nominal values is taken as a systematic uncertainty. Since the B^+ lifetime is known more precisely, its contribution to the uncertainty is neglected.

The effects of the trigger requirements have been evaluated by only using the events triggered by the lifetime unbiased (di)muon lines, which is about 85% of the total number of events. Repeating the complete analysis, a ratio of $R_{c/u} = (0.65 \pm 0.10)\%$ is found, resulting in a systematic uncertainty of 4%.

The tracking uncertainty includes two components. The first is the difference in track reconstruction efficiency between data and simulation, estimated with a tag and probe method [23] of $J/\psi \rightarrow \mu^+ \mu^-$ decays, which is found to be negligible. The second is due to the 2% uncertainty on the effect from hadronic interactions assumed in the detector simulation.

The uncertainty due to the choice of the (p_T, η) binning is found to be negligible. Combining all systematic uncertainties in quadrature, we obtain $R_{c/u} = (0.68 \pm 0.10$ (stat.) ± 0.03 (syst.) ± 0.05 (lifetime))% for B_c^+ and B^+ mesons with transverse momenta $p_T > 4$ GeV/ c and pseudorapidities $2.5 < \eta < 4.5$.

For the mass measurement, different selection criteria are applied. All events are used regardless of the trigger line. The fiducial region requirement is also removed. Only candidates with a good measured mass uncertainty (< 20 MeV/ c^2) are used, and a loose particle identification requirement on the pion of the $B_c^+ \rightarrow J/\psi \pi^+$ decay is introduced to remove the small contamination from $B_c^+ \rightarrow J/\psi K^+$ decays.

The alignment of the tracking system and the calibration of the momentum scale are performed using a sample of $J/\psi \rightarrow \mu^+ \mu^-$ decays in periods corresponding to different running conditions, as described in Ref. [24]. The validity of the calibrated momentum scale has been checked using samples of $K_s^0 \rightarrow \pi^+ \pi^-$ and $\Upsilon \rightarrow \mu^+ \mu^-$ decays. In all cases, the effect of the final state radiation, which cause the fitted masses to be underestimated, is taken into account. The difference between the correction factors determined using the J/ψ and Υ resonances, 0.06%, is taken as the systematic uncertainty.

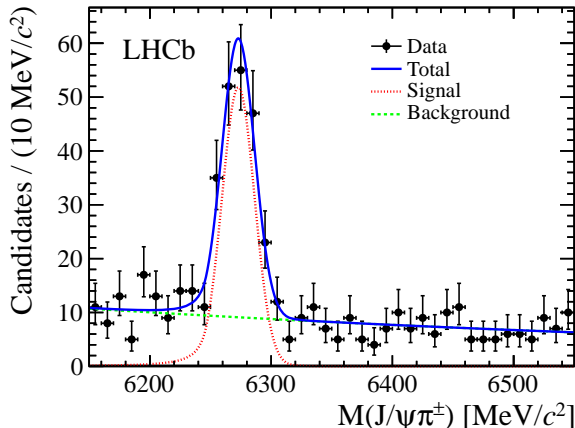


Figure 2: Invariant mass distribution of $B_c^+ \rightarrow J/\psi \pi^+$ decays, used in the mass measurement. The fit to the data is superimposed.

The B_c^+ mass is determined with an extended unbinned maximum likelihood fit to the invariant mass distribution of the selected $B_c^+ \rightarrow J/\psi \pi^+$ candidates. The mass difference $M(B_c^+) - M(B^+)$ is obtained by fitting the invariant mass distributions of the selected $B_c^+ \rightarrow J/\psi \pi^+$ and $B^+ \rightarrow J/\psi K^+$ candidates simultaneously. The fit model is the same as in the production cross-section ratio measurement. Figure 2 shows the invariant mass distribution for $B_c^+ \rightarrow J/\psi \pi^+$. The B_c^+ mass is determined to be $6273.0 \pm 1.3 \text{ MeV}/c^2$, with a resolution of $13.4 \pm 1.1 \text{ MeV}/c^2$, and the mass difference $M(B_c^+) - M(B^+)$ is $994.3 \pm 1.3 \text{ MeV}/c^2$. The uncertainties are statistical only.

The mass measurement is affected by the systematic uncertainties due to the invariant mass model, momentum scale calibration, detector description and alignment. To evaluate the systematic uncertainty, the complete analysis, including the track fit and the momentum scale calibration when needed, is repeated. The parameters to which the mass measurement is sensitive are varied within their uncertainties. The changes in the central values of the masses obtained from the fits relative to the nominal results are then assigned as systematic uncertainties.

Table 1 summarizes the systematic uncertainties assigned to the measured B_c^+ mass and mass difference $\Delta M = M(B_c^+) - M(B^+)$. The main source is the uncertainty in the momentum scale calibration. After the calibration procedure a residual $\pm 0.06\%$ variation of the momentum scale remains as a function of the particle pseudorapidity η . The impact of this variation is evaluated by parameterizing the momentum scale as a function of η . The amount of material traversed by a particle in the tracking system is known to 10% accuracy, the magnitude of the energy loss correction in the reconstruction is therefore varied by 10%. To quantify the effects due to the alignment uncertainty, the horizontal and vertical slopes of the tracks close to the interaction region, which are determined by measurements in the vertex detector, are changed by $\pm 0.1\%$, corresponding to the estimated precision of the length scale along the beam axis [25]. To test the relative alignment of different

Table 1: Systematic uncertainties (in MeV/c^2) of the B_c^+ mass and mass difference $\Delta M = M(B_c^+) - M(B^+)$.

Source of uncertainty	$M(B_c^+)$	ΔM
Mass fitting:		
– Signal model	0.1	0.1
– Background model	0.3	0.2
Momentum scale:		
– Average momentum scale	1.4	0.5
– η dependence	0.3	0.1
Detector description:		
– Energy loss correction	0.1	-
Detector alignment:		
– Vertex detector (track slopes)	0.1	-
– Tracking stations	0.6	0.3
Quadratic sum	1.6	0.6

sub-detectors, the analysis is repeated ignoring the hits of the tracking station between the vertex detector and the magnet. Other uncertainties arise from the signal and background line shapes. The bias due to the final state radiation is studied using a simulation based on PHOTOS [17]. The mass returned by the fit model is found to be underestimated by $0.7 \pm 0.1 \text{ MeV}/c^2$ for the B_c^+ meson, and by $0.4 \pm 0.1 \text{ MeV}/c^2$ for the B^+ meson. The mass and mass difference are corrected accordingly, and the uncertainties are propagated. The effects of the background shape are evaluated by using a constant or a first-order polynomial function instead of the nominal exponential function. The stability of the measured B_c^+ mass is studied by dividing the data samples according to the polarity of the spectrometer magnet and the pion charge. The measured B_c^+ masses are consistent with the nominal result within the statistical uncertainties.

In conclusion, using 0.37 fb^{-1} of data collected in pp collisions at $\sqrt{s} = 7 \text{ TeV}$ by the LHCb experiment, the ratio of the production cross-section times branching fraction of $B_c^+ \rightarrow J/\psi \pi^+$ relative to that for $B^+ \rightarrow J/\psi K^+$ is measured to be $R_{c/u} = (0.68 \pm 0.10 \text{ (stat.)} \pm 0.03 \text{ (syst.)} \pm 0.05 \text{ (lifetime)})\%$ for B_c^+ and B^+ mesons with transverse momenta $p_T > 4 \text{ GeV}/c$ and pseudorapidities $2.5 < \eta < 4.5$. Given the large theoretical uncertainties on both production and branching fractions of the B_c^+ meson, more precise theoretical predictions are required to make a direct comparison with our result. The B_c^+ mass is measured to be $6273.7 \pm 1.3 \text{ (stat.)} \pm 1.6 \text{ (syst.) MeV}/c^2$. The measured mass difference with respect to the B^+ meson is $M(B_c^+) - M(B^+) = 994.6 \pm 1.3 \text{ (stat.)} \pm 0.6 \text{ (syst.) MeV}/c^2$. Taking the world average B^+ mass [10], we obtain $M(B_c^+) = 6273.9 \pm 1.3 \text{ (stat.)} \pm 0.6 \text{ (syst.) MeV}/c^2$, which has a smaller systematic uncertainty. The measured B_c^+ mass is in agreement with previous measurements [5, 6] and a recent prediction given by the lattice QCD calculation, $6278(6)(4) \text{ MeV}/c^2$ [26]. These results represent the most precise determinations of these quantities to date.

Acknowledgements

We express our gratitude to our colleagues in the CERN accelerator departments for the excellent performance of the LHC. We thank the technical and administrative staff at CERN and at the LHCb institutes, and acknowledge support from the National Agencies: CAPES, CNPq, FAPERJ and FINEP (Brazil); CERN; NSFC (China); CNRS/IN2P3 (France); BMBF, DFG, HGF and MPG (Germany); SFI (Ireland); INFN (Italy); FOM and NWO (The Netherlands); SCSR (Poland); ANCS (Romania); MinES of Russia and Rosatom (Russia); MICINN, XuntaGal and GENCAT (Spain); SNSF and SER (Switzerland); NAS Ukraine (Ukraine); STFC (United Kingdom); NSF (USA). We also acknowledge the support received from the ERC under FP7 and the Region Auvergne.

References

- [1] Quarkonium Working Group, N. Brambilla *et al.*, *Heavy quarkonium physics*, arXiv:hep-ph/0412158, and references therein.
- [2] C.-H. Chang and X.-G. Wu, *Uncertainties in estimating hadronic production of the meson B_c and comparisons between TEVATRON and LHC*, Eur. Phys. J. **C38** (2004) 267, arXiv:hep-ph/0309121.
- [3] Y.-N. Gao *et al.*, *Experimental prospects of the B_c studies of the LHCb experiment*, Chin. Phys. Lett. **27** (2010) 061302.
- [4] CDF collaboration, F. Abe *et al.*, *Observation of the B_c meson in $p\bar{p}$ collisions at $\sqrt{s} = 1.8$ TeV*, Phys. Rev. Lett. **81** (1998) 2432, arXiv:hep-ex/9805034; CDF collaboration, F. Abe *et al.*, *Observation of B_c mesons in $p\bar{p}$ collisions at $\sqrt{s} = 1.8$ TeV*, Phys. Rev. **D58** (1998) 112004, arXiv:hep-ex/9804014.
- [5] CDF collaboration, T. Aaltonen *et al.*, *Observation of the decay $B_c^\pm \rightarrow J/\psi\pi^\pm$ and measurement of the B_c^\pm mass*, Phys. Rev. Lett. **100** (2008) 182002, arXiv:0712.1506.
- [6] D0 collaboration, V. M. Abazov *et al.*, *Observation of the B_c meson in the exclusive decay $B_c \rightarrow J/\psi\pi$* , Phys. Rev. Lett. **101** (2008) 012001, arXiv:0802.4258.
- [7] LHCb collaboration, A. A. Alves Jr. *et al.*, *The LHCb detector at the LHC*, JINST **3** (2008) S08005.
- [8] R. Aaij and J. Albrecht, *Muon triggers in the high level trigger of LHCb*, LHCb-PUB-2011-017.
- [9] V. Gligorov, C. Thomas, and M. Williams, *The HLT inclusive B triggers*, LHCb-PUB-2011-016.
- [10] Particle Data Group, J. Beringer *et al.*, *Review of particle physics*, Phys. Rev. **D86** (2012) 010001.

- [11] T. Skwarnicki, *A study of the radiative cascade transitions between the Upsilon-prime and Upsilon resonances*, PhD thesis, Institute of Nuclear Physics, Krakow, 1986, DESY-F31-86-02.
- [12] LHCb collaboration, R. Aaij *et al.*, *Measurements of the branching fractions and CP asymmetries of $B^\pm \rightarrow J/\psi \pi^\pm$ and $B^\pm \rightarrow \psi(2S)\pi^\pm$ decays*, Phys. Rev. **D85** (2012) 091105, [arXiv:1203.3592](#).
- [13] T. Sjöstrand, S. Mrenna, and P. Skands, *PYTHIA 6.4 physics and manual*, JHEP **05** (2006) 026, [arXiv:hep-ph/0603175](#).
- [14] I. Belyaev *et al.*, *Handling of the generation of primary events in GAUSS, the LHCb simulation framework*, Nuclear Science Symposium Conference Record (NSS/MIC) **IEEE** (2010) 1155.
- [15] C.-H. Chang, J.-X. Wang, and X.-G. Wu, *BCVEGPY2.0: An upgraded version of the generator BCVEGPY with the addition of hadroproduction of the P-wave B_c^+ states*, Comput. Phys. Commun. **174** (2006) 241, [arXiv:hep-ph/0504017](#).
- [16] D. J. Lange, *The EvtGen particle decay simulation package*, Nucl. Instrum. Meth. **A462** (2001) 152.
- [17] P. Golonka and Z. Was, *PHOTOS Monte Carlo: A precision tool for QED corrections in Z and W decays*, Eur. Phys. J. **C45** (2006) 97, [arXiv:hep-ph/0506026](#).
- [18] GEANT4 collaboration, J. Allison *et al.*, *Geant4 developments and applications*, IEEE Trans. Nucl. Sci. **53** (2006) 270; GEANT4 collaboration, S. Agostinelli *et al.*, *GEANT4: A simulation toolkit*, Nucl. Instrum. Meth. **A506** (2003) 250.
- [19] M. Clemencic *et al.*, *The LHCb simulation application, GAUSS: design, evolution and experience*, J. of Phys. : Conf. Ser. **331** (2011) 032023.
- [20] M. Pivk and F. R. Le Diberder, *sPlot: A statistical tool to unfold data distributions*, Nucl. Instrum. Meth. **A555** (2005) 356, [arXiv:physics/0402083](#).
- [21] CDF collaboration, A. Abulencia *et al.*, *Measurement of the B_c^+ meson lifetime using $B_c^+ \rightarrow J/\psi e^+ \nu_e$* , Phys. Rev. Lett. **97** (2006) 012002, [arXiv:hep-ex/0603027](#).
- [22] D0 collaboration, V. Abazov *et al.*, *Measurement of the lifetime of the B_c^\pm meson in the semileptonic decay channel*, Phys. Rev. Lett. **102** (2009) 092001, [arXiv:0805.2614](#).
- [23] A. Jaeger *et al.*, *Measurement of the track finding efficiency*, LHCb-PUB-2011-025.
- [24] LHCb collaboration, R. Aaij *et al.*, *Measurement of b-hadron masses*, Phys. Lett. **B708** (2012) 241, [arXiv:1112.4896](#).
- [25] LHCb collaboration, R. Aaij *et al.*, *Measurement of the $B_s^0 - \bar{B}_s^0$ oscillation frequency Δm_s in $B_s^0 \rightarrow D_s^-(3)\pi$ decays*, Phys. Lett. **B709** (2012) 177, [arXiv:1112.4311](#).

- [26] TWQCD Collaboration, T.-W. Chiu and T.-H. Hsieh, *B_s and B_c mesons in lattice QCD with exact chiral symmetry*, PoS **LAT2006** (2007) 180, [arXiv:0704.3495](#).